

Reductive Dechlorination of Trichloroethene and Carbon Tetrachloride Using Iron and Palladized-Iron Cathodes

TIE LI AND JAMES FARRELL*

Department of Chemical and Environmental Engineering,
University of Arizona, Tucson, Arizona 85721

This research investigated the effectiveness of electrochemical reduction for removing trichloroethylene (TCE) and carbon tetrachloride (CT) from dilute aqueous solutions. The kinetics, reaction mechanisms, and current efficiencies for TCE and CT reduction were investigated using flow-through, iron electrode reactors and with amperometric measurements of reduction rates. The electrode reactors were operated over a range of flow rates, pH, ionic strength, dissolved oxygen concentration, and working electrode potentials. Typical reduction half-lives for TCE and CT in the iron reactor were 9.4 and 3.7 min, respectively. The addition of palladium as an electrocatalyst at a level of 1 mg of Pd per m² of electrode surface area increased the reaction rates by a factor of 3. When operated continuously, reaction rates in the palladized-iron reactor were stable over a 9-month period of operation, indicating that there was no loss of palladium from the electrode. In both the iron and Pd–iron reactors, TCE was reduced primarily to ethane and ethene, while CT was reduced almost exclusively to methane. Under all operating conditions, chlorinated compounds accounted for less than 2% of the total reaction byproducts. Comparisons of amperometrically measured current efficiencies with those measured in the flow-through reactors and the weak effect of electrode potential on TCE reaction rates indicated that the primary pathway for TCE reduction by iron and palladized-iron electrodes is indirect and involves atomic hydrogen as the reducing agent. Direct reduction of TCE appeared to be inhibited by the preferential reduction of water. The finding that electrodes coated with a hydrophobic polymer to inhibit water reduction showed current efficiencies greater than 90% for direct TCE reduction supports this hypothesis. For CT, similar amperometric and analytically measured current efficiencies indicated that the primary mechanism for CT reduction is direct electron transfer. Carbon dioxide and bisulfide, which have been found to foul palladium in other catalytic systems, did not deactivate the catalyst. The fast reaction kinetics and electrode stability indicate that electrochemical reduction may be feasible for treating waters contaminated with chlorinated organic compounds.

Introduction

In recent years, there has been considerable interest in developing destructive treatment methods for removing

chlorinated organic compounds from contaminated waters (1–11). Most of these treatment techniques have focused on reductive dechlorination methods that transform chlorinated organic compounds to their nonchlorinated analogues and chloride ions. Reductive dechlorination promoted by zero-valent metals has been a very active research area since Gillham and O'Hannesin (1) proposed that metallic iron filings could be utilized for *in situ* passive groundwater remediation (2–6).

In addition to *in situ* treatment using zero-valent iron, several investigations have reported on reductive dechlorination methods that are fast enough to be employed in above ground canister treatment systems (7–19). Most of these methods use palladium as an electrocatalyst and hydrogen as the reducing agent. The first use of palladium for reductive dechlorination was reported by Muftikian et al. (7), who showed that palladium plated on the surface of zero-valent iron yielded rapid dechlorination rates for trichloroethylene (TCE). However, the effectiveness of the catalyst declines over time due to the buildup of an iron (hydr)oxide film, which obstructs reactant access to the catalytic sites (19).

To avoid the problem of catalyst fouling by iron oxide precipitates, some investigators have used palladium supported on porous alumina or zeolites for reduction of chlorinated and nonchlorinated hydrocarbons (12–15, 18). In one of the earliest studies, Schreier and Reinhard (13) showed that supported palladium catalysts and dissolved hydrogen gas could rapidly dechlorinate aqueous-phase TCE. Other investigators have shown that similar methods were also effective for reductive dechlorination of vapor-phase halocarbons (14).

Although hydrogen gas and supported palladium catalysts rapidly dechlorinate a wide range of halocarbons, the catalysts are readily deactivated by reduced sulfur compounds, carbonate, or carbon dioxide gas (13–15). Deactivation of palladium by carbon dioxide has been attributed to chemisorption of carbon monoxide produced from carbonate reduction (20). Chemisorption of carbon monoxide with the catalyst renders the palladium electron deficient and hinders the dissociative adsorption of molecular hydrogen at the catalyst surface. The mechanisms for sulfur poisoning of palladium catalysts are also well understood and include the following: competitive adsorption of hydrogen sulfide with the reactant species, modification of the electronic properties of the palladium in the vicinity of sulfur atoms, and formation of Pd–S compounds (21–24).

Other investigators have attempted electrochemical reduction of chlorinated aliphatic and aromatic compounds using palladium supported on carbon and graphite cathodes (9, 10, 16, 17). Although rapid dechlorination rates have been achieved with palladium-coated cathodes, the effectiveness of the catalyst is short-lived. Several investigators have reported declining reaction rates over time due to loss of palladium from the electrode (16, 17). The use of solid palladium cathodes eliminates the problem of palladium flaking off the electrode surface. However, a recent investigation reported that a palladium gauze electrode was ineffective for chlorophenol reduction, despite rapid reaction rates by palladium supported on carbon and graphite (10). This result suggests that the mechanisms involved in reductive dechlorination are not well understood.

Halocarbon reduction at cathode surfaces may occur through both direct and indirect mechanisms. Direct reduction may occur by electron tunneling or by formation of a chemisorption complex of the organic compound with the cathode material (25). Electron tunneling may occur to

* Corresponding author phone: (520)621-2465; fax: (520)621-6048; e-mail: farrell@engr.arizona.edu.

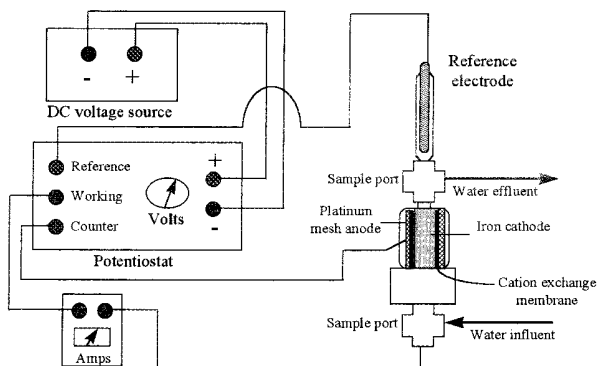


FIGURE 1. Schematic diagram of the electrode reactor and experimental setup.

hydrocarbons that are physically adsorbed at the cathode surface or to compounds that are separated from the cathode surface by adsorbed water or a metal oxide film. Because the probability of electron tunneling to compounds that are not physically adsorbed decreases exponentially with distance from the electrode surface, this mechanism is expected to be insignificant over distances greater than 10 Å (26). Indirect reduction of organic compounds may occur via reaction with atomic hydrogen. Atomic hydrogen adsorbed on the cathode may reduce organic compounds through formation of chemisorbed hydride complexes (25). Reduction by this mechanism is fast on cathodes with low hydrogen overpotentials, such as platinum and palladium, but is much slower on metals with high hydrogen overpotentials, such as iron (25).

The purpose of this research was to investigate the effectiveness of cathodic protection for maintaining the performance of iron and palladium-treated iron for reductive dechlorination of aqueous phase halocarbons and to determine the mechanisms responsible for halocarbon reduction. Reaction rates and byproducts of TCE and carbon tetrachloride (CT) reduction were measured in flow-through, porous iron electrode reactors, with and without the addition of palladium as an electrocatalyst. The effects of elapsed time, pH, ionic strength, dissolved oxygen, electrode potential, and the catalyst poisons (bicarbonate and bisulfide) on TCE and CT dechlorination rates were determined. The mechanisms responsible for TCE and CT reduction were investigated by comparing reaction rates and current efficiencies in the flow-through reactors with amperometric measurements of direct reduction rates.

Materials and Methods

Flow-Through Electrode Experiments. Two flow-through reactors containing porous iron cathodes 2 cm in diameter and 3 cm long were used in the investigation. The electrodes were supplied by Cercona of America (Dayton, OH) and contained 5 wt % aluminosilicate binder and 95% iron. The iron electrodes had a BET (27) measured surface area of approximately 4.5 m² and an internal pore volume of approximately 2 mL. A schematic diagram of the electrode reactors and experimental setup is shown in Figure 1. The anodes consisted of platinum wire screens that were wrapped around the iron cathodes. An ESC-7000 cation exchange membrane (Electrosynthesis Co., Lancaster, NY) was used to separate the anodes and cathodes, and water passed through only the cathode compartment of each reactor. The electrodes were contained within a 2.5 cm o.d. glass tube fitted with stainless steel pipe fittings at each end. The working electrode potentials were set using a potentiostat and saturated calomel electrode. The reactors were operated at cathodic potentials ranging from -755 to -1200 mV with

respect to the standard hydrogen electrode (SHE). All potentials are reported with respect to the SHE.

Except where indicated, the reactors were operated using a 3 mM CaSO₄ background electrolyte solution that was deoxygenated by purging with nitrogen gas. The effect of ionic strength on reaction rates was investigated by adding 100 mM NaCl to the background electrolyte solution. The effects of dissolved oxygen and carbonate on reaction rates were investigated by purging the feedwater with 15 mL/min of air or carbon dioxide. Potential catalyst deactivation by reduced sulfur compounds was investigated by adding 1 mM Na₂S to the feedwater. The palladized-iron electrodes were prepared by passing a tetraamminepalladium(II) chloride solution through the reactor to achieve a palladium loading of 1.0 mg/m².

Influent and effluent concentrations of TCE and CT were measured by extracting 50-μL aqueous samples into 1 g of pentane. Analytes in the pentane were then quantified by injection into a Hewlett-Packard 5890 gas chromatograph equipped with an electron capture detector and an autosampler. Nonchlorinated reaction byproducts were measured by injecting 500-μL aqueous samples into a counter-current stripping apparatus purged with nitrogen gas. The analytes stripped into the purge gas were then quantified using a molecular sieve column mounted in a SRI Instruments gas chromatograph equipped with a flame ionization detector (FID). Trace reaction byproducts such as chloroform, methylene chloride, and dichloroethylene isomers were identified using a Finnigan ITD 700 gas chromatograph/mass spectrometer. Dissolved iron and palladium concentrations were determined by the Soil, Water and Plant Analysis Laboratory at the University of Arizona, using inductively coupled plasma mass spectroscopy. X-ray diffraction analyses of the electrodes were performed by the Geosciences X-ray Diffraction Laboratory at the University of Arizona.

Amperometric Analyses. Amperometric analyses using chronoamperometry were performed in a custom three-electrode cell using an EG&G (Oak Ridge, TN) model 273A potentiostat and M270 software. All experiments utilized a Ag/AgCl reference electrode and a platinum wire counter electrode. An iron disk (Metal Samples Company, Munford, AL), and iron, platinum, and palladium wires (Aesar, Ward Hill, MA) were used as working electrodes. Supporting electrolyte solutions were deoxygenated prior to use by purging with argon. An EG&G model 616 rotating disk electrode was used to amperometrically measure CT reduction rates and current efficiencies over a range of CT concentrations and electrode potentials. Electrode currents were independent of the rotation rate for speeds greater than 1000 rpm. Current efficiencies and reaction rates were determined by comparing electrode currents in blank electrolyte solutions and those containing CT.

Results and Discussion

Zero-valent iron is thermodynamically unstable in water and must be cathodically protected in order to prevent anodic dissolution of the iron. The potential (E_H) required to prevent anodic dissolution depends on the ferrous iron activity [Fe²⁺] as given by the Nernst equation at 25 °C (28):

$$E_H = -0.440 + 0.0295 \log [\text{Fe}^{2+}] \quad (1)$$

Although cathodic protection can minimize anodic dissolution of the iron, cathodic polarization cannot prevent the formation of an oxide coating on the electrode surface. Since the feed solutions used in this study contained no dissolved iron, anodic dissolution of the electrodes occurred until a visible oxide formed on the electrode surfaces. During the first day of operation, formation of the oxide was evident by a change in electrode color from metallic silver to black.

TABLE 1. Half-Lives with 95% Confidence Intervals for CT and TCE Reduction at a Cathode Potential of -755 mV, Neutral pH, and Influent Concentrations of 0.12 and 0.28 mM, Respectively^a

compd	iron reactor half-life (min)	Pd–iron reactor half-life (min)	iron reactor k_{sa} ($L m^{-2} h^{-1}$)	iron filings (3) k_{sa} ($L m^{-2} h^{-1}$)
CT	3.7 ± 0.2	1.3 ± 0.1	5.6×10^{-3}	5×10^{-3} to 0.5
TCE	9.4 ± 1.5	2.7 ± 0.2	2.2×10^{-3}	6×10^{-5} to 0.03

^a Also listed are normalized first-order reaction rate constants for CT and TCE reduction in the iron electrode reactor and literature values for CT and TCE reduction by zero-valent iron filings.

Subsequent X-ray diffraction analysis of the surface oxide from one electrode indicated that it was composed of magnetite. To eliminate the effects of changing electrode surface chemistry on halocarbon reaction rates, all measurements were taken after equilibrating the electrodes with the solutions for at least 1 day.

The reactors were operated at cathode potentials ranging from -755 to -1200 mV. Although this potential range is below the stability domain of water, visible amounts of hydrogen gas were observed only at potentials below -900 mV. The low rate of hydrogen production can be attributed to the high overpotential of the hydrogen evolution reaction on iron and iron oxide surfaces (26). Over the range of potentials investigated, the degree of cathodic protection was sufficient to maintain constant reaction rates in both the palladized and the untreated iron reactors over a 9-month period of continuous operation. Dissolved iron concentrations in the reactor effluent were below the detection limit of $60 \mu\text{g/L}$. Within the limits of experimental precision, effluent pH values were the same as influent values.

Both mass transfer and reaction rate limitations may affect the degree of reactant conversion in flow-through reactors. Under all operating conditions, the performance of the electrode reactors was well described by a plug flow, packed-bed reactor model with a first-order reaction rate (29). For all the kinetic data reported in this investigation, the reactors were operated at flow rates where mass transfer limitations and dispersion effects on reactant conversion were negligible. At low flow rates, where the hydraulic residence time was greater than 4 min, preliminary testing indicated that reaction rates increased with increasing flow rate in quantitative accord with boundary layer mass transfer theory for packed-bed reactors (29). However, at hydraulic residence times shorter than 2 min, the effect of mass transfer limitations on reaction rates was negligible.

Over the concentration range investigated (0.1–1.2 mM), reaction rates were first-order in reactant concentration. Therefore, the reaction rates can be characterized in terms of a single parameter, such as a first-order rate constant (k) or the reactant half-life (29). Table 1 compares reaction rates for TCE and CT in the untreated and palladized-iron reactors at hydraulic residence times of 1–2 min and a cathode potential of -755 mV. In the iron reactor, the half-lives for TCE and CT were 9.4 ± 1.5 and 3.7 ± 0.2 min, respectively. Palladium treatment at a level of 1 mg/m^2 reduced the TCE half-life to 2.7 ± 0.2 min and the CT half-life to 1.3 ± 0.1 min. These reaction rates can be compared to rates in other systems by normalizing the observed k by the surface area to solution volume in the reactor, as in $k_{sa} = k(V/\sigma)$; where V is the pore volume of the reactor and σ is the reactive surface area of the electrode. In Table 1, the surface area normalized rate constants (k_{sa}) for the iron reactor are compared to those previously reported (3) for CT and TCE reduction by zero-valent iron filings. For both CT and TCE,

the electrode k_{sa} values are within the range of those reported for reduction by zero-valent iron. This suggests that there is not a substantial increase in reaction rates due to cathodic protection of the iron. However, reaction rates in the electrode reactors did not show the declining performance over time that has been observed with zero-valent iron filings (6, 30).

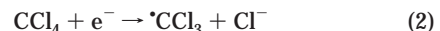
Small performance differences were observed between different electrodes due to variations in electrode surface area and pore volume. Therefore, comparisons of reaction rates under different operating conditions can only be made for reactors using the same electrode. Removal of the palladized-iron electrodes from the reactor resulted in a partial loss of catalytic activity upon subsequent use. This loss in catalytic activity was due to the buildup of iron oxides on top of the palladium, similar to that observed for palladized-iron filings (19).

Reaction Byproducts and Pathways. The reaction byproducts for TCE reduction by cathodically protected iron and palladized iron were similar to those reported for reduction by zero-valent iron (4). In both the iron and palladized-iron reactors, ethane and ethene accounted for more than 95% of the TCE reaction byproducts, with acetylene accounting for up to 5%. Carbon mass balances of more than 90% were obtained, and trace amounts of the three dichloroethene isomers, vinyl chloride, 1-butene, and 2-butene were also detected. Under all experimental conditions, the sum of all chlorinated byproducts accounted for less than 1% of the TCE that was reduced. The exact ratio of the two major byproducts varied by $\pm 20\%$ depending on the flow rate, with lower flow rates favoring greater ethane production.

The observed distribution of reaction byproducts suggests that the β -elimination mechanism proposed by Roberts et al. (5) is the primary reaction pathway. The β -elimination pathway involves a two-electron transfer to produce chloroacetylene from TCE. The resulting chloroacetylene then undergoes hydrogenolysis to form acetylene which then undergoes another two-electron transfer to form ethene. Although no chloroacetylene was detected in any experiments, the absence of this intermediate product has been explained by its rapid reaction rate (6).

Methane was the major reaction product of CT reduction in both the iron and palladized-iron reactors and accounted for more than 95% of the CT that was transformed. The chlorinated byproducts (chloroform and methylene chloride) together accounted for less than 2% of the transformed CT. The low yield of chlorinated byproducts from CT reduction contrasts with reports of near-stoichiometric production of chloroform for CT reduction by zero-valent iron (4).

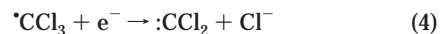
Previous investigators have reported that cathodic reduction of CT initiates with a one-electron transfer to form a trichloromethyl radical as given by (31)



For reduction by zero-valent iron, the trichloromethyl radical is normally reduced to chloroform as in (4)



However, a second pathway exists in which the trichloromethyl radical is reduced to dichlorocarbene and a chloride ion as given by (32)



The dichlorocarbene is then hydrolyzed to give CO and HCl. Thus, the second pathway illustrated by eq 4 does not produce chlorinated daughter products from CT reduction. The high yield of methane suggests that CO is rapidly reduced in the reactors.

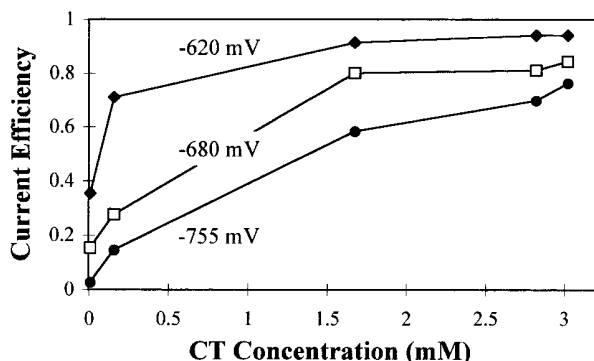


FIGURE 2. Amperometrically determined current efficiencies for CT reduction by an iron rotating disk electrode as a function of electrode potential and CT concentration.

Previous investigators have reported that the reaction 4 pathway becomes more favored the lower the potential of the reducer (33). The near-absence of chlorinated products supports this reaction pathway. Because of the small degree of reactant conversion (~50%), if CT reduction produced chloroform followed by methylene chloride, these products should have been present at significant yields due to their slower reaction rates as compared to CT. In independent tests with each halocarbon, the rate constants for chloroform and methylene chloride were smaller than the rate constant for CT by factors of 3.5 and 26, respectively.

Current Efficiency. Comparisons of amperometrically measured current efficiencies, defined as the fraction of the total cell current going toward halocarbon reduction, with current efficiencies in the electrode reactor can be used to determine the relative contributions of direct and indirect reduction. Dehalogenation of compounds for which the reduction mechanism is direct can be measured amperometrically by comparing currents in blank electrolyte solutions to those with added halocarbons. In contrast, indirect reduction by atomic hydrogen cannot be detected amperometrically but can be determined from the extent of halocarbon reduction in the electrode reactors. Amperometrically measured current efficiencies for CT reduction by a rotating disk electrode are shown in Figure 2 as a function of the CT concentration and electrode potential. The current efficiency for CT reduction increases with increasing CT concentration and decreases with decreasing electrode potential. The high current efficiencies for direct CT reduction at an aqueous concentration of 3 mM indicate that CT reduction is more favorable than water reduction. This conclusion is also supported by high current efficiencies measured for CT reduction by iron wire electrodes in solutions saturated with CT. At an electrode potential of -680 mV, a current efficiency of 94% was measured for CT reduction using potential step chronoamperometry. The high current efficiency was obtained despite a low adsorbed phase concentration of CT. Anson analysis (34) of the early time chronoamperometry profile indicated that the fraction of the electrode surface covered with CT was only 18%, based on the nominal geometric surface area of the electrode. However, due to molecular scale roughness, the actual electrode surface area was greater than its geometric surface area; therefore, the actual adsorbed surface coverage by CT was even smaller than 18%.

The current efficiencies for CT reduction in the iron electrode reactor were close to those measured amperometrically using the rotating disk electrode. Agreement of the amperometric and analytically determined current efficiencies indicates that the predominant mechanism for CT reduction involves direct electron transfer from the electrode.

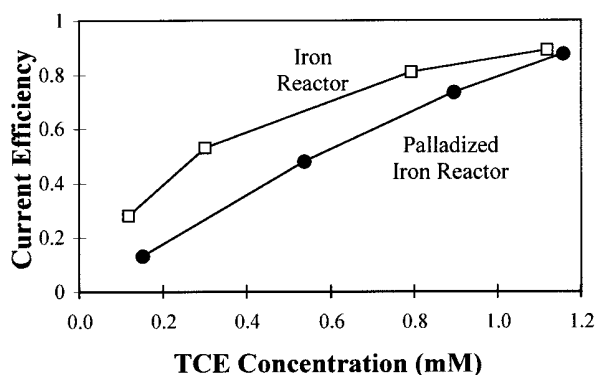


FIGURE 3. Current efficiency for TCE reduction in the iron and palladized-iron reactors at an electrode potential of -755 mV and a hydraulic residence time of 1.4 min.

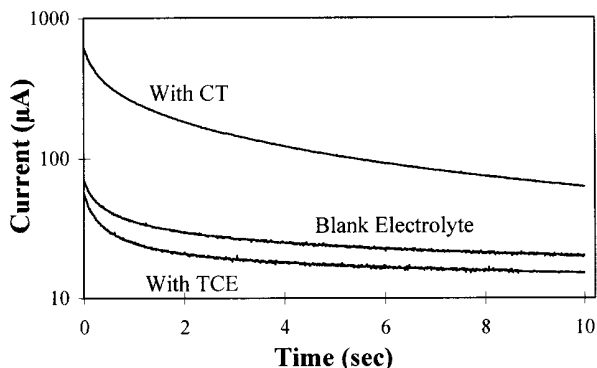


FIGURE 4. Chronoamperometric profiles at a potential of -780 mV for a palladium wire electrode in a blank 10 mM CaSO_4 solution and in 10 mM CaSO_4 solutions saturated with TCE or CT.

The current efficiencies for TCE reduction at an electrode potential of -755 mV in the iron and palladized-iron reactors are shown in Figure 3. The data in Figure 3 show that the current efficiency for TCE reduction by the iron electrode is greater than 90% at a TCE concentration of 1 mM. At this same concentration and electrode potential of -755 mV, the data in Figure 2 show that the current efficiency for CT reduction is only 38%. The high current efficiency for TCE is surprising given that TCE reduction cannot be measured amperometrically using the rotating disk electrode or by potential step chronoamperometry. Iron and platinum wire electrodes polarized to -780 mV in solutions saturated with TCE give the same currents as those polarized in blank electrolyte solutions. This indicates that TCE reduction is indirect and occurs via reaction with atomic hydrogen stored in the electrode.

Potential step amperometric analysis of TCE reduction by a palladium wire electrode indicates that TCE reduction by palladized iron is also indirect. Figure 4 shows chronoamperometry profiles for TCE and CT reduction by a palladium wire electrode immersed in 3 mM CaSO_4 solutions, with and without added halocarbons. In the TCE-saturated electrolyte solution, the steady-state current was 25% smaller than the current in the blank electrolyte solution. This indicates that adsorption of TCE blocks reduction of water. In contrast, adding CT to the electrolyte solution resulted in an order of magnitude increase in the initial current before mass transfer limitations became a factor. This indicates that CT can be directly reduced by the palladium wire. Experiments analytically measuring TCE reduction by the palladium wire electrode found that the k_{sa} of $1.3 \times 10^{-3} \text{ L m}^{-2} \text{ h}^{-1}$ was a factor of 2 smaller than the k_{sa} for TCE reduction in the iron electrode reactor and more than 600 times smaller than the

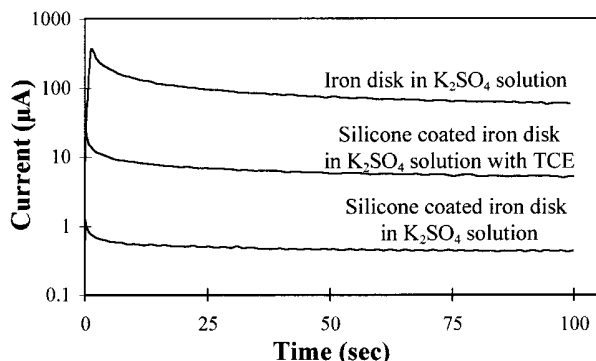


FIGURE 5. Chronoamperometric profiles for an iron disk electrode, with and without a hydrophobic silicone surface coating, at a potential of -780 mV in 100 mM K_2SO_4 solutions.

k_{sa} for CT reduction by the palladium wire. The slow reduction rate of TCE by the palladium wire electrode suggests that the reaction rate enhancement by palladium supported on iron is due to its strong adsorption of TCE, which then allows indirect reduction by atomic hydrogen.

The absence of significant direct TCE reduction by iron, platinum, and palladium wire electrodes can most likely be attributed to preferential reduction of water at the electrode surface. If this is the case, then coating the electrode with a hydrophobic material should decrease water reduction and allow amperometric measurement of direct TCE reduction. This hypothesis was tested by coating an iron disk electrode with silicone vacuum grease and measuring chronoamperometry profiles in 100 mM K_2SO_4 solutions, with and without TCE. As shown in Figure 5, coating the electrode with a hydrophobic polymer reduced the steady-state current associated with water reduction from 60 to 0.43 μ A. However, after adding TCE to the solution, the steady-state current increased from 0.43 to 5.1 μ A. This corresponds to a current efficiency of 92% for TCE reduction and indicates that inhibition of water reduction can lead to direct reduction of TCE.

Effect of Electrode Potential. The effect of electrode potential on TCE reaction rates in the flow-through reactors can be used to assess the contribution of direct electron transfer to the overall rate of TCE reduction. In the absence of mass transfer limitations, the potential dependence of electrochemical reaction rates can be described by the Butler–Volmer equation (26):

$$i = i_0 [e^{-\bar{\alpha}F(E-E_{eq})/RT} - e^{\bar{\alpha}F(E-E_{eq})/RT}] \quad (5)$$

where i is net current associated with the reaction, i_0 is the exchange current, F is the Faraday constant, R is the gas constant, T is the temperature, E is the potential of the electrode, E_{eq} is the equilibrium potential for the redox reaction, and $\bar{\alpha}$ and $\bar{\alpha}$ are the transfer coefficients for the reduction and oxidation reactions, respectively. The first term in brackets gives the rate of the forward reduction reaction, while the second term gives the rate of the reverse oxidation reaction. The transfer coefficients depend on the number of electrons transferred before and after the rate-determining step and whether the rate-determining step is limited by chemical- or potential-dependent factors (26). Since reductive dechlorination reactions are not reversible, the E_{eq} for a particular reaction cannot be measured directly but can be estimated from thermodynamic data for reactant and product species (5). At neutral pH and a chloride activity of 10^{-3} M, the equilibrium potential for a two-electron reduction of TCE to chloroacetylene has been estimated to be 599 mV (5). Therefore, the potentials used for TCE reduction in this investigation were sufficiently below the E_{eq} that the term

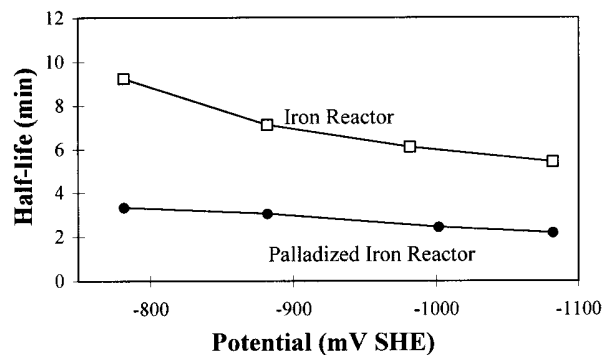


FIGURE 6. Effect of electrode potential on the half-life of TCE in the iron and palladized-iron reactors at a hydraulic residence time of 1.4 min and influent concentration of 0.28 mM.

TABLE 2. Effect of pH of the Reduction Half-Lives of CT and TCE at an Electrode Potential of -755 mV and Influent Concentrations of 0.26 and 0.24 mM, Respectively

pH	TCE half-life (min)		CT half-life (min)	
	iron	Pd–iron	iron	Pd–iron
4	5.5 ± 0.3	3.8 ± 0.2	1.5 ± 0.1	1.3 ± 0.1
7	6.2 ± 0.4	4.5 ± 0.2	3.6 ± 0.2	1.5 ± 0.1
10	16.8 ± 3.0	6.0 ± 0.4	3.0 ± 0.2	1.7 ± 0.1

representing the rate of the reverse reaction in eq 5 is negligible as compared with the term accounting for the forward reduction reaction. Therefore, the effect of electrode potential on the TCE reduction rate constant (k_r) should be described by

$$k_r = k_0 e^{-\bar{\alpha}F(E-E_{eq})/RT} \quad (6)$$

where k_0 is the standard rate constant, which is dependent on only chemical factors. Thus, according to eq 6, the ratio of reaction rate constants at two electrode potentials, E_1 and E_2 , is then given by

$$k_{r1}/k_{r2} = e^{-\bar{\alpha}F(E_1-E_2)/RT} \quad (7)$$

The effect of electrode potential on TCE reaction rates in the iron and palladized-iron reactors is shown in Figure 6. In the iron reactor, decreasing the electrode potential resulted in small increases in the TCE reaction rate. However, the increases in reaction rate were less than expected based on the behavior predicted by eq 7. To evaluate eq 7, the transfer coefficient must be known. For a multistep, multiple electron-transfer reaction in which the rate-determining step is potential dependent, the minimum value of the transfer coefficient is close to 0.5 (26). Taking the reaction rate constant at -782 mV as k_{r1} and $\bar{\alpha}$, the rate constant, k_{r2} , at -0.882 mV should be a factor of 49 times greater than that at -782 mV, if the reaction rate-limiting step involves electron transfer. However, the measured reaction rate constant for TCE increased by only 23% between -0.782 and -0.882 mV. The small potential dependence of the TCE reaction rate indicates that the rate-limiting step for TCE reduction does not involve electron transfer or that the primary TCE reduction pathway is indirect. A similar conclusion can be made for TCE reduction in the palladized-iron reactor.

Water Chemistry Effects. The effect of pH on reaction rates was investigated by comparing TCE and CT reduction rates in solutions with pH values of 4 , 7 , and 10 . As shown by the data in Table 2 for the iron reactor, the reduction half-life for TCE increased by a factor of 3 between pH 4 and pH 10 . Smaller pH effects were observed for TCE reduction

in the palladized-iron reactor. The greater pH effect in the untreated iron reactor supports the conclusion that molecular hydrogen is involved in TCE reduction by the iron electrode. Although the higher pH values contribute to decreased cathodic production of hydrogen in both the untreated and palladized-iron reactors, the palladium serves to concentrate the available hydrogen, thereby reducing the influence of pH on reaction rates. The effects of pH on CT reduction in the palladized-iron reactor were small, and there was no consistent trend in the iron electrode reactor. The small pH effects are consistent with a reaction mechanism involving direct CT reduction.

Because oxygen is more facilely reduced than either CT or TCE, oxygen reduction may compete with reduction of the target compounds. To investigate this possibility, TCE and CT reaction rates in the palladized-iron reactor were measured in solutions with dissolved oxygen concentrations of 0 and 9 mg/L. At an electrode potential of -755 mV, adding oxygen to the feedwater resulted in an increase in the cell current from 11 to 18 mA but did not affect the rates of TCE or CT reduction. This indicates that there were no competitive effects with dissolved oxygen for reactive sites on the electrode surface. Tests comparing reaction rates in 3 mM CaSO_4 and 100 mM NaCl solutions indicated that reaction rates were also independent of the background electrolyte solution.

The effect of carbonate species on palladium deactivation was investigated by comparing TCE reaction rates in feedwaters with and without dissolved carbon dioxide. Purging the feedwater with carbon dioxide gas resulted in an $\text{H}_2\text{CO}_3(\text{aq})$ concentration of 31.6 mM at a pH of 4.3. Bicarbonate and carbonate levels were 0.32 mM and 3.2×10^{-4} μM , respectively. After 4 days of operation with carbon dioxide in the feed stream at an electrode potential of -755 mV and a hydraulic residence time of 1 min, the reaction rate for TCE was the same as that before addition of carbon dioxide. This indicates that dissolved carbon dioxide does not deactivate the palladium catalyst. The addition of carbon dioxide did increase the cell current from 11 to 16 mA, mostly due to increased hydrogen evolution resulting from the lower pH value of the influent solution. However, some of the increase in current was due to reduction of carbon dioxide itself. The reaction products of carbon dioxide reduction were determined after removing TCE from the feed stream. Carbon dioxide reduction produced methane, ethane, and ethylene. These are similar to the reaction products previously reported for reduction of carbon dioxide by zero-valent iron (35).

Complete reduction of carbon dioxide to hydrocarbons may explain the absence of poisoning effects by carbon monoxide. In this experiment, polarization of the electrode maintained the palladium at sufficiently negative potentials to reduce carbon monoxide completely to hydrocarbons. However, in catalytic systems where dissolved hydrogen is the electron donor, the low aqueous solubility of hydrogen gas may not produce sufficiently negative cathodic potentials to completely reduce carbon monoxide.

To test the effect of reduced sulfur compounds on catalyst poisoning, the palladized-iron reactor was operated at a potential of -780 mV for 4 days with a feedwater containing 0.44 mM HS^- and 0.56 mM H_2S . Addition of the sulfide increased the TCE half-life in the palladized-iron reactor from 3.8 ± 0.2 to 5.2 ± 0.3 min. However, upon removing sulfide from the feed stream, the TCE half-life recovered to 3.6 ± 0.2 min, indicating that that sulfide did not permanently deactivate the palladium catalyst. The slower reaction rate in the presence of sulfide can likely be attributed to competitive adsorption of H_2S on the palladium (21–23).

The fast reaction rates and electrode stability observed in this investigation indicate that cathodic reduction may be a practical process for treating waters contaminated with chlorinated organic compounds. Although iron is a base metal

that forms an oxide coating even under cathodic polarization, it may be a practical electrode material due to its low cost and high overpotential for hydrogen evolution. At the electrode potentials used in this investigation, noble metal cathodes, such as platinum and palladium, would produce more than 2 orders of magnitude more hydrogen per unit surface area of electrode (36). Furthermore, noble metal cathodes are highly susceptible to deactivation by deposition of metallic impurities, whereas oxide-coated electrodes are much less susceptible to deactivation (37). Although the performance enhancement of the palladium catalyst may have been limited by mass transfer effects associated with reactant diffusion through a surface oxide layer, the fast reaction rates in the untreated iron reactor indicate that precious metal catalysts may not be necessary to achieve practically feasible halocarbon reduction rates.

Acknowledgments

Although the research described in this paper has been funded in part by the United States Environmental Protection Agency through Grant R-825223-01-0 to J.F., it has not been subjected to the Agency's required peer and policy review and therefore does not necessarily reflect the views of the Agency, and no official endorsement should be inferred. Additional funding was provided by Dames and Moore and Research Corporation Technologies. Thanks to Rich Helferich at Cercon of America and Bill Bostick at Midwest Research Institute for providing the electrodes.

Literature Cited

- Gillham, R. W.; O'Hannesin, S. F. *Modern Trends in Hydrology*; International Association of Hydrologists Conference; IAH: Hamilton, ON, Canada, 1992; pp 10–13.
- Gillham, R. W.; O'Hannesin, S. F. *Ground Water* **1994**, *32*, 958.
- Tratnyek, P. G.; Johnson, T. L.; Scherer, M. M.; Eykholt, G. R. *Ground Water Monit. Remed.* **1997**, *108*.
- Matheson, L. J.; Tratnyek, P. G. *Environ. Sci. Technol.* **1994**, *28*, 2045.
- Roberts, A. L.; Totten, L. A.; Arnold, W. A.; Burris, D. R.; Campbell, T. J. *Environ. Sci. Technol.* **1996**, *30*, 2654.
- Campbell, T. J.; Burris, D. R.; Roberts, A. L.; Well, J. R. *Environ. Toxicol. Chem.* **1997**, *16* (4), 625.
- Muftikian, R.; Fernando, Q.; Korte, N. *Water Res.* **1995**, *29*, 2434.
- Zhang, W.; Wang, C. *Abstracts of Papers*, 213th National Meeting of the American Chemical Society, San Francisco; American Chemical Society: Washington, DC, 1997; Vol. 37 (1), p 78.
- Neurath, S. A.; Ferguson, W. J.; Dean, S. B.; Foose, D.; Agrawal, A. *Abstracts of Papers*, 213th National Meeting of the American Chemical Society, San Francisco; American Chemical Society: Washington, DC, 1997; Vol. 37 (1), p 159.
- Cheng, I. F.; Fernando, Q.; Korte, N. *Environ. Sci. Technol.* **1997**, *31*, 1074.
- Siantar, D. P.; Schreier, C. G.; Chou, C.; Reinhard, M. *Water Res.* **1996**, *30*, 2315.
- Schuth, C.; Reinhard, M. *Appl. Catal. B: Environ.* **1998**, *18*, 215.
- Schreier, C. G.; Reinhard, M. *Chemosphere* **1995**, *31* (6), 3475.
- McNab, W. W.; Ruiz, R. *Chemosphere* **1998**, *37* (5), 925–936.
- Munakata, N.; McNab, W.; Haag, W.; Roberts, P. V.; Reinhard, M. *Abstracts of Papers*, 213th National Meeting of the American Chemical Society, San Francisco; American Chemical Society: Washington, DC, 1997; Vol. 37 (1), p 168.
- Lyon, J. M. *Abstracts of Papers*, 213th National Meeting of the American Chemical Society, San Francisco; American Chemical Society: Washington, DC, 1997; Vol. 37 (1), p 143.
- Helvenston, M. C.; Presley, R. W.; Zhao, B. *Abstracts of Papers*, 213th National Meeting of the American Chemical Society, San Francisco; American Chemical Society: Washington, DC, 1997; Vol. 37 (1), p 294.
- Lowry, G. V.; Reinhard, M. *Environ. Sci. Technol.* **1999**, *33*, 1905.
- Muftikian, R.; Nebesny, K.; Fernando, Q.; Korte, N. *Environ. Sci. Technol.* **1996**, *30*, 3593–3596.
- Spessard, G. O.; Miessler, G. L. *Organometallic Chemistry*; Prentice Hall: Englewood Cliffs, NJ, 1997.
- Hegedus, L. L.; McCabe, R. W. *Catalyst Poisoning*; Marcel Dekker: New York, 1984.

- (22) Angel, G. D.; Benitez, J. L. *J. Mol. Catal.* **1994**, 409.
- (23) Wilke, S.; Scheffler, M. *Surf. Sci.* **1995**, 329, L605–L610.
- (24) Hughes, R. *Deactivation of Catalysts*; Academic Press: London, 1984.
- (25) Brewster, J. H. *J. Am. Chem. Soc.* **1954**, 76, 6361.
- (26) Bockris, J. O'M.; Reddy, A. K. *Modern Electrochemistry*, Vol. 2; Plenum Press: New York, 1970.
- (27) Brunauer, S.; Emmett, P. H.; Teller, E. *J. Am. Chem. Soc.* **1938**, 60, 309.
- (28) Pourbaix, M. *Atlas of Electrochemical Equilibria*; Pergamon Press: Oxford, 1966.
- (29) Fogler, H. S. *Elements of Chemical Reaction Engineering*, 3rd ed.; Prentice Hall: Upper Saddle River, NJ, 1999.
- (30) Schreier, C. G.; Reinhard, M. *Chemosphere* **1994**, 29 (8), 1743.
- (31) Saveant, J. M. In *Advances in Physical Organic Chemistry*, Vol. 26; Bethell, D., Ed.; Academic Press: London, 1990.
- (32) Robinson, E. A. *J. Am. Chem. Soc.* **1961**, 1663.
- (33) Balko, B.; Tratnyek, P. G. *J. Phys. Chem. B* **1998**, 102, 1459–1465.
- (34) Bard, A. J.; Faulkner, L. R. *Electrochemical Methods*; John Wiley and Sons: New York, 1980.
- (35) Hardy, L. I.; Gillham, R. W. *Environ. Sci. Technol.* **1996**, 30, 57.
- (36) Dole, M. *Principles of Experimental and Theoretical Electrochemistry*; McGraw-Hill: New York, 1935.
- (37) Trasatti, S. In *Electrochemistry of Novel Materials*; Lipkowski, J., Ross, P. N., Eds.; VCH Publishers: New York, 1994; Chapter 5.

Received for review July 1, 1999. Revised manuscript received October 18, 1999. Accepted October 25, 1999.

ES9907358